HHS Public Access

Author manuscript

J Magn Reson Imaging. Author manuscript; available in PMC 2017 December 01.

Published in final edited form as:

J Magn Reson Imaging. 2016 December ; 44(6): 1474–1482. doi:10.1002/jmri.25304.

Prospective frequency correction for macromolecule suppressed GABA editing experiments at 3T

Richard A. E. Edden, Ph.D.[1,2], **Georg Oeltzschner, Ph.D.**[1,2], **Ashley D. Harris, Ph.D.**[1,2,3,4,5], **Nicolaas A. J. Puts, Ph.D.**[1,2], **Kimberly Chan, B.Sc.**[1,2,6], **Vincent O. Boer, Ph.D.**[7], **Michael Schär, Ph.D.**[1], and **Peter B. Barker, D.Phil.**[1,2]

[1]Russell H. Morgan Department of Radiology and Radiological Science, The Johns Hopkins University School of Medicine, Baltimore, MD

[2]F.M. Kirby Center for Functional Brain Imaging, Kennedy Krieger Institute, Baltimore, MD

[3]CAIR Program, Alberta Children's Hospital Research Institute, University of Calgary, AB, Canada

[4]Department of Radiology, University of Calgary, AB, Canada

[5]Hotchkiss Brain Institute and Alberta Children's Hospital Research Institute, Calgary, AB, Canada

[6]Department of Biomedical Engineering, The Johns Hopkins University School of Medicine, Baltimore, MD

[7]Hvidovre Hospital, Danish Research Center for Magnetic Resonance, Hvidovre, Denmark

Abstract

Purpose—‘Symmetric’ editing schemes have been proposed to suppress unwanted co-edited MM signals in GABA editing. To investigate the effects of B_0 field offsets and drift on macromolecule (MM) suppressed GABA-editing experiments, and to implement and test a prospective correction scheme.

Methods—Full density-matrix simulations of both conventional (non-symmetric) and symmetric MM-suppressed editing schemes were performed for the GABA spin system to evaluate their offset-dependence. Phantom and *in vivo* (15 subjects at 3T) GABA-edited experiments with symmetrical suppression of macromolecular (MM) signals were performed to quantify the effects of field offsets on the total GABA+MM signal (designated as GABA+). A prospective frequency correction method based on interleaved water referencing (IWR) acquisitions was implemented and its experimental performance evaluated during positive and negative drift.

Results—Simulations show that the signal from MM-suppressed symmetrical editing schemes is an order of magnitude more susceptible to field offsets than the signal from non-symmetric editing schemes. The MM-suppressed GABA signal changes by 8.6% per Hz for small field offsets. IWR significantly reduces variance in the field offset and measured GABA levels (both $p<0.001$ by F-tests) the scanner offset, maintaining symmetric suppression of MM signal.

Corresponding Author: Richard A. E. Edden, 600 N Wolfe Street, Park 367H, Baltimore, MD 21287., 410 614 3418, raee2@jhu.edu.

Conclusions—Symmetrical editing schemes substantially increase the dependence of measurements on B_0 field offsets, which can arise due to patient movement and/or scanner instability. It is recommended that symmetrical editing should be used in combination with effective B_0 stabilization, such as that provided by interleaved water referencing.

Keywords

Symmetrical editing; GABA; MM-suppressed; B0 drift; instability; field-frequency lock

INTRODUCTION

J-difference editing is a widely used method for selectively detecting lower-concentration metabolites in ^{1}H magnetic resonance spectra of the *in vivo* brain (1,2). It has been used to detect compounds such as gamma-aminobutyric acid (GABA), lactate, glutathione, ascorbate, and N-acetyl aspartyl glutamate (NAAG) (3–9). The J-difference method uses selective radiofrequency pulses applied to a specific resonance within the molecule of interest in order to remove modulation due to J-coupling. Two experiments are performed with and without the application of the selective pulses (usually called the ON and OFF experiments), and the difference between these two yields a spectrum which only contains those signals that are affected by the editing pulse.

Unfavorably, difference spectra often contain co-edited signals from species that have a coupling network which is similar to the target molecule. In the case of GABA editing (10,11), the selectivity is limited by the required echo time (TE) which is usually set to 68 ms (due to the triplet-like structure of the 3-ppm signal (12)). Because of this limited selectivity, editing pulses applied to the 1.9 ppm GABA resonance also partially invert macromolecular (MM) resonances at 1.7 ppm that are coupled to MM signals at 3 ppm. Thus, the detected signal at 3 ppm contains a contribution of as much as 50% from MM, depending on acquisition parameters (10), and is therefore referred to as ‘GABA+’ to reflect the contributions from both GABA and MM.

The co-edited MM signal can be suppressed by using a ‘symmetric-editing’ scheme where the frequencies of the ON/OFF editing pulses are set to 1.9 and 1.5 ppm respectively, i.e. placed symmetrically around the MM resonance at 1.7 ppm, and the selectivity of the editing pulses is increased (7,13). However, the use of more selective pulses, and the requirement for symmetry, makes the experiment more sensitive to experimental imperfections, and in particular makes it very sensitive to frequency changes due to drift (or miscalibration) of the main B_0 field. B_0 field instability may occur due to patient movement, gradient-induced heating or cooling and/or superconducting magnet instability. In conventional single-voxel MRS, field instability results in increased linewidths; in edited experiments, it can cause both increased linewidths as well as imperfect subtraction of signals in OFF and ON spectra resulting in subtraction artifacts in the spectra. Both these problems can be addressed by retrospective frequency-and-phase correction before signal averaging (14–16). However, B_0 field changes will also change the efficiency of the editing, and result in imperfect symmetric suppression of nulled contaminants, which can *not* be corrected retrospectively. Therefore, prospective frequency correction during data acquisition is desirable to spectral-

editing experiments when frequency drift is comparable to or greater than the bandwidth of the editing pulses.

Prospective field-frequency locking has long been used to improve B_0 stability in high-resolution nuclear magnetic resonance (NMR) spectroscopy, and, to a lesser extent, in *in vivo* MR spectroscopy. It entails maintaining a consistent B_0 magnetic field through constant feedback by utilizing the signal of deuterated solvents (17), fluorine field probes outside the body (18), or intrinsic water from volume-localized (19,20) and non-localized (21) interleaved navigator scans.

Selective, symmetrical editing for GABA is one *in vivo* application where frequency-field locking is likely to show substantial benefits. The purpose of this paper is to investigate the effects of B_0 field offsets and drift on macromolecule (MM) suppressed GABA-editing experiments, and to implement and test a prospective correction scheme.

METHODS

Simulations Of Field Offset In GABA+ And MM-suppressed Experiments

To establish the change in editing efficiency over a range of B_0 field offsets, density-matrix simulations of resonances were performed for the GABA spin system, using the 'FID-A' package, a MATLAB-toolbox for simulation and analysis of MRS data (12). FID-A propagates the density matrix through each step of the MEGA-PRESS experiment, and then calculates the observable terms to simulate an FID signal.

Simulations of two distinct MEGA-PRESS experiments were run for a B_0 field strength of 3T: a) the classic 'MM-unsuppressed' 'GABA+' editing scheme (TE = 68 ms), which applies 14-ms editing pulses at 1.90 ppm in ON scans and at 7.46 ppm in OFF scans; and b) the 'MM-suppressed' scheme (TE = 80 ms), which applies 20-ms editing pulses at 1.90 ppm in ON scans and 1.50 ppm in OFF scans (13). Simulations for both experiments used sinc-Gaussian editing pulses, an ideal 90° excitation pulse (rotation around the x-axis), and amplitude-modulated slice-selective refocusing pulses. The chemical shifts and coupling constants of the GABA system were taken from recent literature (12). All simulations were performed for the center of the voxel only (i.e. without separate consideration of a spatial matrix).

To investigate the effects of field drift on editing performance, simulations were run with field offsets ranging from −1.00 ppm to +1.00 ppm with increments of 0.02 ppm. The editing efficiency function of GABA was subsequently created by plotting the integral of the 3 ppm GABA triplet over the field offset. For both experiments, the co-editing efficiency function of the MM signal was modeled by shifting this GABA editing efficiency function by 0.2 ppm, since the identity of the MM spin system is not agreed upon And has not been parameterized. Effects of field offset were only calculated for the editing pulses; for slice-selective pulses with bandwidth over 1 kHz, the effects of drift are minor.

Under typical conditions, the MM and GABA contributions to the 'GABA+' signal are believed to be approximately equal (10), allowing relative normalization of the MM and

GABA signal curves at zero field offset. The total edited signal at a range of offsets can then be calculated from the sum of the respective GABA and MM contributions. This same normalization factor (1.21), which relates to the different *in vivo* abundance of GABA and MM, was applied for simulations of the MM-suppressed experiment.

Phantom Measurements

To assess the reliability of the simulations, MM-suppressed GABA-edited MEGA-PRESS measurements were carried out on a phosphate-buffered saline phantom (1 liter) containing 10 mM GABA. Scans were performed on a Philips Achieva 3T scanner using body coil for RF transmit and an 8-channel phased array head coil for receive. Acquisition parameters include: 20 ms editing pulses during a TE of 80 ms (13), 30×30×30 mm^3 voxel; 32 averages; 16-step phase-cycle; 2k datapoints sampled at a spectral width of 2 kHz; TR 2s. Editing pulses were applied at 1.9 and 1.5 ppm. To imitate the effect of field offsets on editing, the difference between these editing pulse frequencies was maintained (at 0.4 ppm) and an offset series was performed so that the editing frequencies were varied from 2.9/2.5 ppm to 0.9/0.5 ppm in increments of 0.05 ppm.

These phantom experiments investigate the changes seen in GABA editing, but if shift by 0.2 ppm will approximate the changes seen in MM suppression. Such a proxy is necessary, since no phantom MM preparation has been validated for MRS.

In Vivo Measurements

Implementation of prospective frequency-field locking using interleaved water referencing (IWR) was achieved without an increase in overall scan time by re-ordering the acquisition of water-suppressed GABA-edited data and non-water-suppressed reference data. Rather than acquiring 16 averages (one full phase cycle) of water reference data at the start of the acquisition, as is typically done for eddy-current correction and quantification, these reference acquisitions were dispersed throughout the acquisition, as shown in Figure 1. Each interleaved PRESS water reference scan was acquired with a full acquisition window (2048 datapoints sampled at 2 kHz). These data were Fourier transformed with eightfold zero-filling in real-time on the scanner. The frequency difference between the magnitude maximum and the center of the spectrum was used to determine the frequency offset, which was then automatically added to the spectrometer center frequency prior to the next set of water-suppressed acquisitions. Hence, the frequencies of all pulses (including localization and editing pulses) were prospectively updated in an automated fashion.

Fifteen adult subjects were recruited to this study, which was approved by the institutional review board, and after obtaining written informed consent. An MM-suppressed GABA-edited MEGA-PRESS scan was set up for all *in vivo* experiments. Two in vivo experiments were performed on a Philips Achieva 3T scanner using body coil for RF transmit and a 32-channel phased array head coil for receive, and share the following core parameters: 20 ms editing pulses applied during a TE of 80 ms (13); 35×35×35 mm^3 midline parietal voxel; 320 averages of water-suppressed (using VAPOR (22)) data and 16 averages of water reference data (acquiring a full phase cycle, so that water-suppressed and water reference data are co-localized); 2k datapoints sampled at a spectral width of 2 kHz; TR 2s.

Experiment 1: In Vivo Offset Series—In three subjects, the relationship between the *in vivo* edited MM-suppressed GABA signal and the field offset was investigated. Analogous to the phantom measurements, an *in vivo* offset series was acquired in three healthy adult subjects (2F, 1M). The field offset series was performed by varying the pair of editing pulse frequencies within a range of 2.25/1.85 ppm to 1.4/1.0 ppm, sampling offsets of 0.5, 0.45, 0.4, 0.32, 0.25, 0,15, 0.07, 0.0, −0.1, −0.18, −0.25 and −0.35 ppm; of the 12 experiments, four were acquired in each subject.

Experiment 2: Interleaved Water Referencing—The efficacy of IWR for reducing B_0 field offset and maintaining symmetry of MM suppression *in vivo* was investigated. MM-suppressed MEGA-PRESS data were acquired in twelve healthy participants (9F, 3M) with editing pulses applied at 1.9 and 1.5 ppm. Two acquisitions were made for each participant, one with interleaved water referencing on (IWR-ON) and one with interleaved water referencing off (IWR-OFF). Data were acquired under natural (i.e. that induced by the prior scanner user, without special intervention), varying field drift conditions. In one case, the preceding hour included multiple echo-planar and/or diffusion tensor (EPI/DTI) acquisitions known to cause gradient heating. All *in vivo* data were processed using the 'Gannet' program (23), which, amongst other functions, gives estimates of the field offset during the time-course of the experiment, derived for the changes determined by post-processing frequency alignment. GABA levels were quantified relative to the unsuppressed water signal from the same volume (reported in 'institutional units', i.u.), by fitting a Gaussian model to the GABA signal at 3 ppm and a Gaussian-Lorentzian to the water signal.

Frequency offset data from the interleaved water-reference method were also processed to establish the accuracy of corrections. The frequency of each transient was again determined from the Gannet output.

In order to infer the size of the applied correction, the difference in water frequency between the water-suppressed scans directly before and directly after the correction can be multiplied by 1.1. This adjustment corrects for the fact that the difference in offset between scans either side of the correction is the sum of the correction itself and any drift that occurs during that TR. The offset prior to each correction was plotted against the correction made.

To demonstrate the impact of IWR on measured GABA levels, the 3.0 ppm peak area was plotted against the mean field offset for the IWR-ON and IWR-OFF conditions.

Statistical Methods

Correlations were quantified using Pearson's Correlation Coefficient. Student's t-tests were performed to test for group differences, e.g. in measured GABA levels with and without IWR. An F-test was used to test for group-differences in variance, e.g. in measured GABA levels with and without IWR. P-values < 0.05 associated with these tests were considered significant.

RESULTS

Simulations And Phantom Measurements

Density-matrix simulations of the edited GABA signal as a function of B_0 offset in the GABA+ experiment (i.e. not MM-suppressed with 14-ms editing pulses) are shown in Figure 2A. The inversion profile of the sinc-Gaussian editing pulse used is overlaid, demonstrating that the two curves are very similar between offsets of +1 to −0.5 ppm. The approximately Gaussian function is maximal for GABA on-resonance, so that the signal of GABA changes fairly slowly for small field offsets. Slight deviations between the two functions only occur for large negative field offsets, when the editing pulse starts to directly saturate the detected 3 ppm GABA protons frequency.

The simulated field offset dependence of the GABA signal for the MM-suppressed experiment is shown in Figure 2B, demonstrating excellent agreement with phantom data. This experiment has a two-lobed editing efficiency profile, as signals can either be inverted by the editing pulse in ON scans or in OFF scans. Since these two are subtracted, the two lobes have opposite polarity, with ON-inverted signals positive and OFF-inverted signals negative. The optimal editing efficiency for GABA is slightly shifted from zero field offset due to the small effect from the wing of the OFF pulse centered at 1.5 ppm.

The offset-dependence of GABA and MM in the MM-unsuppressed experiment are shown in Figure 3A. The GABA and MM curves are calibrated to be equal at zero field offset as described in the methods section, achieved by applying a 1.21 y-scaling to the MM curve relative to the GABA curve. The editing efficiency of MM at zero field offset is approximately 70% of its maximum, and MM signal increases for positive offsets, i.e. as the resonant frequency of the 1.7 ppm spins (which changes with B_0) moves closer to the frequency of the editing pulses (which remains constant). The total GABA+ signal (i.e. GABA+MM) is maximal at an offset of +0.08 ppm.

The offset-dependence of the MM-suppressed experiment for GABA and MM is presented in Figure 3B, using the two-lobed editing profile from Figure 2B. With zero field offset, the MM function is at a zero-point, as required, with positive field offsets resulting in positive MM co-editing and negative offsets resulting in negative MM co-editing. The sum of the GABA and MM curves, which is the experimental signal detected, is relatively steep at zero offset, reflecting the rapid changes in MM signal that occur around its zero-crossing. The MM function is again scaled by 1.21 relative to the GABA function for normalization of GABA:MM (50:50 ratio at zero offset). Dashed lines indicate the total signal curves for slightly different GABA:MM ratios, namely a slightly steeper slope for 45:55 GABA:MM, and a slightly shallower slope for 55:45 GABA:MM.

Figure 3C shows the % signal GABA+MM signal change as a function of field offset for the MM-unsuppressed (Figure 3A) and MM-suppressed (Figure 3B) simulations, showing the much greater dependence of the MM-suppressed signal on field offset. The slope of the MM-suppressed line at zero field offset corresponds to a signal change of −8.6% per Hz of field offset, whereas the slope of the MM-unsuppressed line at zero field offset corresponds to a signal change of only −0.86% per Hz of field offset. In both experiments, GABA curves

show relatively small slopes around zero field offset. It is the rapid modulation of MM co-editing with the field offset that is responsible for the increased B_0 sensitivity of the MM-suppressed signal. A 'typical' field drift of ±4 Hz (~ 0.03 ppm) will induce signal changes of about ±30% for the MM-suppressed experiment, versus only about ±3% for the MM-unsuppressed experiment.

In Vivo Experiments

The effect of B_0 field offset on the total *in vivo* signal of the MM-suppressed MEGA-PRESS experiment is shown in Figure 4. The experimental data points are in reasonable agreement with the simulation plot for a 50:50 GABA:MM ratio, demonstrating considerable variance of the total signal over the given offset range. It can be seen that positive field offsets induce a substantial positive MM contribution to the GABA peak. Negative offsets may cause the GABA and MM contributions to cancel each other out, and can even lead to negative total signal. Spectra corresponding to such large positive and negative total offset are displayed as insets.

The effect of IWR frequency-field locking on water frequency stability during MEGA-PRESS is shown in Figure 5. In one case, excessive drift (~46 Hz over 10 minutes) was caused by acquiring MRS data after a prior session of EPI/DTI scanning, as seen in Figure 5A, whereas in the IWR-ON condition drift is limited to a maximum of 6.4 Hz (Figure 5B). The sawtooth pattern of linear drifts and periodic frequency updates is clearly seen in Figure 5B. IWR frequency correction keeps the scanner frequency substantially closer to resonance than the uncorrected case. Substantial drift leads to altered editing of both the GABA and MM peak (editing pulses are no longer on resonance) leading to an apparently negative 'GABA' peak in this case (Figure 5C). Comparison of water frequency offset for IWR-OFF and IWR-ON (Figure 5A vs. Figure 5B) shows significantly more variability in the total water frequency drift over the whole acquisition in the IWR-OFF condition (6.5 ± 12.1 Hz) than in the IWR-ON (1.4 ± 0.9 Hz; F-test fstat 192.3, $p < 0.001$). After exclusion of the acquisition with extreme drift and its IWR-ON counterpart, this significant difference was maintained (IWR-OFF: 2.74 ± 2.12 Hz; IWR-ON: 1.19 ± 0.57 Hz, F-test fstat 14.2, $p < 0.001$). There was no significant difference in mean GABA levels between IWR-OFF and IWR-ON acquisitions ($p=0.5$), but there was significantly more variability in the IWR-OFF group (standard deviation IWR-OFF 1.34 and IWR-ON 0.19, $p < 0.001$). However, variability did not differ significantly after removal of the large drift scan (standard deviation IWR-OFF 0.25 and IWR-ON 0.19, $p = 0.4$).

Figure 5D shows the accuracy of the frequency corrections from the stabilized experiments in Figures 5A–C, demonstrating a very strong linear relationship (Pearson, $R = -0.92$, $p < 0.001$) between the required correction, i.e. the field offset one TR before the interleaved water acquisition (traced from the Spectral Registration routine incorporated in Gannet), and the size of the correction that is actually performed.

Furthermore, the measured GABA levels for each participant were significantly correlated with the frequency drift in the IWR-OFF condition (white circles in Figure 5E, Pearson correlation: $R^2 = 0.77$, $p = 0.008$ with the extreme negative GABA point removed) so that participants with positive drift in the IWR-OFF condition showed an increase in measured

GABA values compared to the IWR-ON condition (with corrected drift) and participants with negative drift in the IWR-OFF condition showing a decrease in measured GABA levels compared to the IWR-ON condition. Plotting the measured GABA levels against the frequency drift in the IWR-ON condition (black circles in Figure 5E), the relationship is much weaker (Pearson correlation: $R^2 = 0.19$, $p = 0.16$).

DISCUSSION

Symmetrical spectral editing is an elegant pulse sequence motif that allows a co-edited signal to be removed from edited spectra, augmenting the selectivity of the editing pulses themselves. Critical to its success is the requirement that editing pulses be placed at equal offsets, positive and negative, in ON and OFF scans relative to the co-editing resonance. This symmetry is broken by changes in the scanner frequency that arise due to subject movement and temperature-related scanner drift, or if scanner frequency is not correctly calibrated. The results in this paper clearly indicate that, for MM-suppressed measurements of GABA using the symmetrical editing scheme, the changes in measured GABA signal that arise from this loss of symmetry are substantial for magnitudes of field drift that can be commonly encountered on clinical scanners, i.e. several Hz. Symmetrical MM-suppression substantially increases the offset-dependence of edited measurements compared to conventional MM-unsuppressed measurements.

Simulations indicate that the increased sensitivity to frequency changes arises from nulling the macromolecular signal, as the MM editing efficiency function has a relatively steep slope at its null point. Standard MM-unsuppressed editing benefits in two ways from less selective editing pulses: the GABA signal is more forgiving of frequency changes; and the MM editing efficiency function has an almost 5-fold lower slope around zero field offset. The net result is that the total signal from the MM-suppressed experiment may be as much as 10 times more susceptible to frequency. The consequence is a relative signal change as high as 8.6% per Hz-off-resonance originating from the imperfectly suppressed MM signal. While the additional positive MM contribution from positive field offset reaches a maximum at +0.12 ppm (+15 Hz), the negative total signal slope continues until it reaches a minimum at −0.34 ppm (−43 Hz). Field drift of this order of magnitude can be seen on clinical scanners quite routinely after gradient-intensive imaging sequences (such as DTI) that cause extensive gradient heating and subsequent cooling during the lower duty cycle MRS acquisition. As the main motivation of removing MM signal from the GABA+ signal is to remove MM-related variance, such an experiment will be unsuccessful unless it is performed with effective frequency stabilization. The direct benefit of IWR for MM-suppressed measurements of GABA is demonstrated by the *in vivo* data presented. While under typical drift conditions there were no significant differences in GABA measurements associated with the interleaved water reference, because measurements increase or decrease based on the direction of drift, a strong correlation existed between the drift and the GABA measurement in the non-IWR scans, but not with IWR correction. IWR substantially reduced the impact of drift on the GABA measurements.

Estimates of signal change for the MM-suppressed experiment has been based upon MM:GABA ratios that result in a signal ratio of 1:1 for the GABA+ editing scheme.

However, it has been shown that the contribution of MM may vary substantially between brain regions and/or subjects (24), as might the GABA signal. In case of higher MM:GABA ratios, the steep slope of the MM signal envelope will tend to increase the susceptibility of MM-suppressed GABA estimates to field offsets.

The numerical results presented here represent one particular implementation of MM-suppressed GABA editing. Based on these results, prospective field-frequency locking can be expected to generally enhance the selectivity of any edited MRS experiment that relies on symmetrical suppression of co-edited resonances. The degree of benefit arising from field-frequency locking will depend on the co-editing behavior of the particular systems involved, which can be specifically determined by applying the template of simulations, and phantom and in vivo experiments. The key factors are the selectivity of the editing pulses (i.e. their duration, power and shape), the separation of the chemical shifts of the resonances involved, and also the B_0 field strength. Field-frequency locking will be especially important when the symmetrically suppressed compound is of substantially higher concentration, as is the case for symmetrical suppression of NAA for edited detection of NAAG (4). Unless prospective field-frequency locking is employed, positive or negative NAA co-editing is likely to bias NAAG estimates in an even more severe manner than co-editing of MM affects GABA. Field-frequency locking is also expected to improve conventional (i.e. non-symmetric) editing experiments that also use highly selective editing pulses (25,26). These results are presented in the context of GABA editing at 3T, the most widely used field strength for editing. At higher field strengths, the selectivity of editing pulses increases (in ppm terms) and at 7T, it is possible to edit GABA with substantial co-editing of MM without symmetrical editing. Care should be taken in making predictions for other field strengths based on these results.

Prospective field-frequency locking is not a new idea, but implementation *in vivo* is not widespread and still has challenges. Small flip-angle approaches that can be performed during every TR are in principle desirable as they do not increase scan time, and would allow for frequency update every TR. However, the accurate and rapid determination of voxel frequency within-TR remains challenging. However, such measurements are typically performed on a whole slice, rather than the localized volume, since the signal from a localized STEAM or PRESS sequence with small flip angles is very small. For single-voxel applications in which shimming of the voxel is achieved using high-order shim coils, the average frequency over the whole slice (or the whole volume) may not be a good indicator of the frequency within the localized voxel for MRS. In such cases, slice-selective frequency stabilization may well provide an erroneous correction for the localized voxel. The influence of lipid signal on such whole-slice methods is also unpredictable. Voxel-localized frequency correction is more likely to return the correct frequency offset, and has been implemented to be accurate enough to reduce offset effects even in situations of mild drift and/or motion, without loss of temporal SNR caused by additional acquisitions. Prior reports of interleaved water-reference acquisition have generally acquired one reference per TR, gaining additional temporal resolution of the lock at the expense of increased scan times (19,20).

Tracking of B_0 frequency can in principal be carried out with different methods. Other than the additional interleaved acquisition of the internal water signal, it may be possible to

extract the field drift directly from the metabolite spectra, e.g. using the Cr peak as a reference (27). While doing so may reduce the acquisition time and be applied every TR, fitting the Cr signal on-line will be computationally demanding as well as complex to implement. Moreover, with edited measurements increasingly being performed on smaller volumes, the SNR of the Cr peak in a single FID may not be sufficient for accurate determination of field offsets. Other real-time motion/frequency correction approaches include external optical motion tracking (28) and rapid 2D field mapping during acquisition (29), either requiring additional hardware or complex sequence implementation. Lastly, an additional benefit of the proposed interleaved internal water acquisition that may outweigh the ~30s time penalty lies in its potential use for concentration estimation and eddy-current correction (10). If substantial abrupt subject motion is expected rather than or on top of mild drift and/or motion, it may be required to implement real-time shim update routines, which have been proposed for edited MRS (30) and edited 3D MRSI (31) of GABA. A recent report (32) has investigated the impact of drift on GABA+, suggesting discarding edited scans with more than 15 Hz drift.

There are a number of limitations to the design of this study, including its reliance on simulations and phantoms of GABA to infer the quality of MM suppression, low subject numbers, lack of patients, and lack of independent validation.

In conclusion, the aim of measuring GABA concentration without contamination from co-edited MM signal is clearly desirable. However, symmetrical suppression experiments with highly selective editing pulses fail relatively rapidly as field drift occurs, reintroducing the possibility of MM-associated variance (either positive or negative), with increased susceptibility to subject motion. For this reason, we recommend that symmetrical editing with MM suppression be applied in combination with effective frequency stabilization on scanners equipped with high-power gradient systems that lead to more than 0.1–0.2 Hz/min field drift, or for studies where group differences in motion are possible.

Acknowledgments

Grant Support: This work was supported by NIH grants R01 EB016089, P41 015909, R21 NS077300, R21 MH 098228, and Ro1 MH106564.

References

1. Rothman DL, Petroff OA, Behar KL, Mattson RH. Localized 1H NMR measurements of gamma-aminobutyric acid in human brain in vivo. Proc. Natl. Acad. Sci. U. S. A. 1993; 90:5662–5666. [PubMed: 8516315]
2. Mescher M, Merkle H, Kirsch J, Garwood M, Gruetter R. Simultaneous in vivo spectral editing and water suppression. NMR Biomed. 1998; 11:266–272. [PubMed: 9802468]
3. Terpstra M, Henry P-G, Gruetter R. Measurement of reduced glutathione (GSH) in human brain using LCModel analysis of difference-edited spectra. Magn. Reson. Med. 2003; 50:19–23. [PubMed: 12815674]
4. Edden RAE, Pomper MG, Barker PB. In vivo differentiation of N-acetyl aspartyl glutamate from N-acetyl aspartate at 3 Tesla. Magn. Reson. Med. 2007; 57:977–982. [PubMed: 17534922]
5. Star-Lack J, Spielman D, Adalsteinsson E, Kurhanewicz J, Terris DJ, Vigneron DB. In Vivo Lactate Editing with Simultaneous Detection of Choline, Creatine, NAA, and Lipid Singlets at 1.5 T Using

PRESS Excitation with Applications to the Study of Brain and Head and Neck Tumors. J. Magn. Reson. 1998; 133:243–254. [PubMed: 9716465]

6. Edden RAE, Schär M, Hillis AE, Barker PB. Optimized detection of lactate at high fields using inner volume saturation. Magn. Reson. Med. 2006; 56:912–917. [PubMed: 16964614]
7. Henry P-G, Dautry C, Hantraye P, Bloch G. Brain GABA editing without macromolecule contamination. Magn. Reson. Med. 2001; 45:517–520. [PubMed: 11241712]
8. Edden RAE, Barker PB. Spatial effects in the detection of γ-aminobutyric acid: Improved sensitivity at high fields using inner volume saturation. Magn. Reson. Med. 2007; 58:1276–1282. [PubMed: 17969062]
9. Emir UE, Raatz S, McPherson S, Hodges JS, Torkelson C, Tawfik P, White T, Terpstra M. Noninvasive quantification of ascorbate and glutathione concentration in the elderly human brain. NMR Biomed. 2011; 24:888–894. [PubMed: 21834011]
10. Mullins PG, McGonigle DJ, O'Gorman RL, Puts NAJ, Vidyasagar R, Evans CJ, Edden RAE. Current practice in the use of MEGA-PRESS spectroscopy for the detection of GABA. NeuroImage. 2014; 86:43–52. [PubMed: 23246994]
11. Puts NAJ, Edden RAE. In vivo magnetic resonance spectroscopy of GABA: A methodological review. Prog. Nucl. Magn. Reson. Spectrosc. 2012; 60:29–41. [PubMed: 22293397]
12. Near J, Evans CJ, Puts NAJ, Barker PB, Edden RAE. J-difference editing of gamma-aminobutyric acid (GABA): Simulated and experimental multiplet patterns. Magn. Reson. Med. 2013; 70:1183–1191. [PubMed: 23213033]
13. Edden RAE, Puts NAJ, Barker PB. Macromolecule-suppressed GABA-edited magnetic resonance spectroscopy at 3T. Magn. Reson. Med. 2012; 68:657–661. [PubMed: 22777748]
14. Evans CJ, Puts NAJ, Robson SE, Boy F, McGonigle DJ, Sumner P, Singh KD, Edden RAE. Subtraction artifacts and frequency (Mis-)alignment in J-difference GABA editing. J. Magn. Reson. Imaging. 2013; 38:970–975. [PubMed: 23188759]
15. Harris AD, Glaubitz B, Near J, John Evans C, Puts NAJ, Schmidt-Wilcke T, Tegenthoff M, Barker PB, Edden RAE. Impact of frequency drift on gamma-aminobutyric acid-edited MR spectroscopy. Magn. Reson. Med. 2014; 72:941–948. [PubMed: 24407931]
16. Near J, Edden R, Evans CJ, Paquin R, Harris A, Jezzard P. Frequency and phase drift correction of magnetic resonance spectroscopy data by spectral registration in the time domain. Magn. Reson. Med. 2014; 73:44–50. [PubMed: 24436292]
17. Hoult DI, Richards RE, Styles P. A novel field-frequency lock for a superconducting spectrometer. J. Magn. Reson. 1978; 30:351–365.
18. Wilm BJ, Duerst Y, Dietrich BE, Wyss M, Vannesjo SJ, Schmid T, Brunner DO, Barmet C, Pruessmann KP. Feedback field control improves linewidths in in vivo magnetic resonance spectroscopy. Magn. Reson. Med. 2014; 71:1657–1662. [PubMed: 23798466]
19. Thiel T, Czisch M, Elbel GK, Hennig J. Phase coherent averaging in magnetic resonance spectroscopy using interleaved navigator scans: Compensation of motion artifacts and magnetic field instabilities. Magn. Reson. Med. 2002; 47:1077–1082. [PubMed: 12111954]
20. Lange T, Zaitsev M, Buechert M. Correction of frequency drifts induced by gradient heating in 1H spectra using interleaved reference spectroscopy. J. Magn. Reson. Imaging. 2011; 33:748–754. [PubMed: 21563261]
21. Henry PG, van de Moortele P-F, Giacomini E, Nauerth A, Bloch G. Field-frequency locked in vivo proton MRS on a whole-body spectrometer. Magn. Reson. Med. 1999; 42:636–642. [PubMed: 10502751]
22. Tkáč I, Starčuk Z, Choi I-Y, Gruetter R. In vivo 1H NMR spectroscopy of rat brain at 1 ms echo time. Magn. Reson. Med. 1999; 41:649–656. [PubMed: 10332839]
23. Edden RAE, Puts NAJ, Harris AD, Barker PB, Evans CJ. Gannet: A batch-processing tool for the quantitative analysis of gamma-aminobutyric acid–edited MR spectroscopy spectra. J. Magn. Reson. Imaging. 2014; 40:1445–1452. [PubMed: 25548816]
24. Harris AD, Puts NAJ, Barker PB, Edden RAE. Spectral-editing measurements of GABA in the human brain with and without macromolecule suppression. Magn. Reson. Med. 2014; 74:1523–1529. [PubMed: 25521836]

25. Terpstra M, Marjanska M, Henry P-G, Tkáč I, Gruetter R. Detection of an antioxidant profile in the human brain in vivo via double editing with MEGA-PRESS. Magn. Reson. Med. 2006; 56:1192–1199. [PubMed: 17089366]

26. Wijnen JP, Haarsma J, Boer VO, Luijten PR, van der Stigchel S, Neggers SFW, Klomp DWJ. Detection of lactate in the striatum without contamination of macromolecules by J-difference editing MRS at 7 T. NMR Biomed. 2015; 28:514–522. [PubMed: 25802216]

27. Waddell KW, Avison MJ, Joers JM, Gore JC. A practical guide to robust detection of GABA in human brain by J-difference spectroscopy at 3 T using a standard volume coil. Magn. Reson. Imaging. 2007; 25:1032–1038. [PubMed: 17707165]

28. Zaitsev M, Speck O, Hennig J, Büchert M. Single-voxel MRS with prospective motion correction and retrospective frequency correction. NMR Biomed. 2010; 23:325–332. [PubMed: 20101605]

29. Keating B, Ernst T. Real-time dynamic frequency and shim correction for single-voxel magnetic resonance spectroscopy. Magn. Reson. Med. 2012; 68:1339–1345. [PubMed: 22851160]

30. Saleh MG, Alhamud A, Near J, van der Kouwe AJW, Meintjes EM. Volumetric navigated MEGA-SPECIAL for real-time motion and shim corrected GABA editing. NMR Biomed. 2015 (Epub ahead of print).

31. Bogner W, Gagoski B, Hess AT, et al. 3D GABA imaging with real-time motion correction, shim update and reacquisition of adiabatic spiral MRSI. NeuroImage. 2014; 103:290–302. [PubMed: 25255945]

32. Tsai SY, Fang CH, Wu TY, Lin YR. Effects of Frequency Drift on the Quantification of Gamma-Aminobutyric Acid Using MEGA-PRESS. Sci Rep. 2016 Apr 15.6:24564. [PubMed: 27079873]

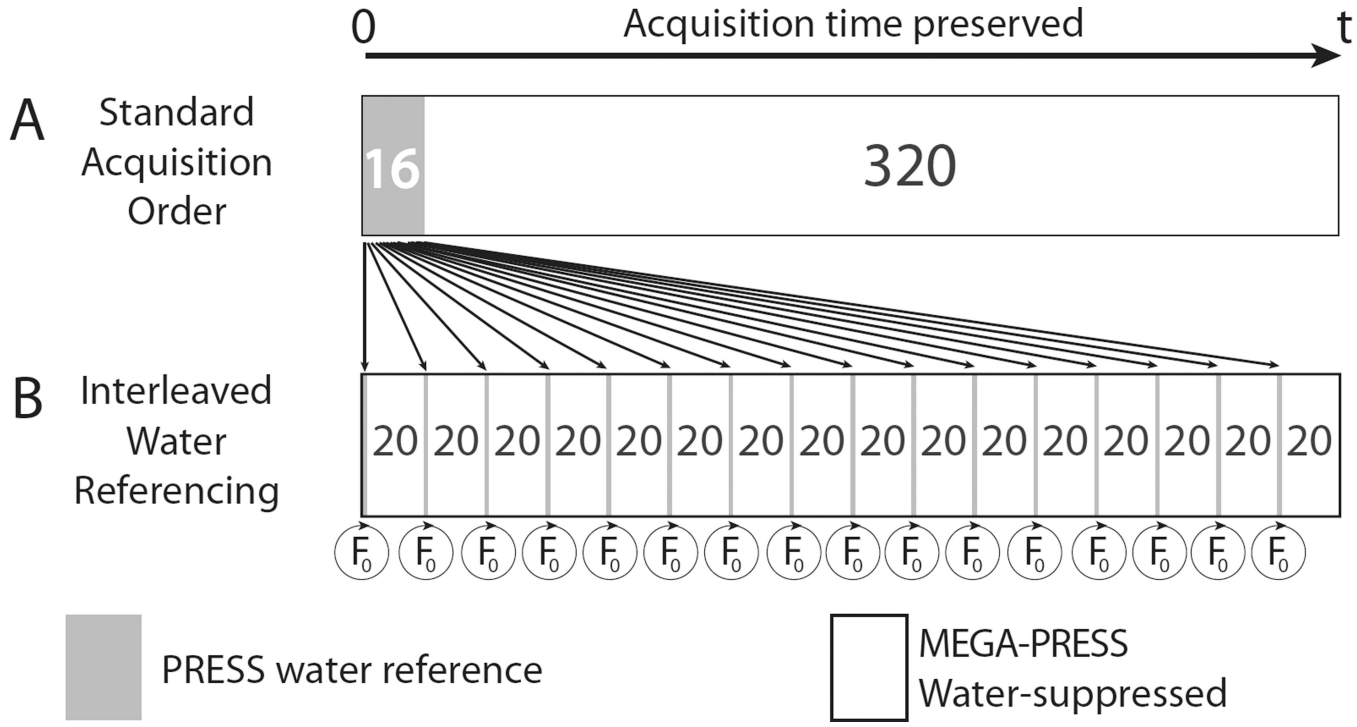

Figure 1.

Schematic diagram of the Interleaved Water Reference (IWR) acquisition scheme. (A) Typically, the 16 water-reference scans are acquired *en bloc* before the 320 water-suppressed scans. (B) In the IWR scheme, the same number of water-reference TRs can be distributed throughout the acquisition (1 for every 20 water-suppressed scans) without changing the total acquisition time, allowing accurate determination of the field offset and periodic F_0 update during the scan.

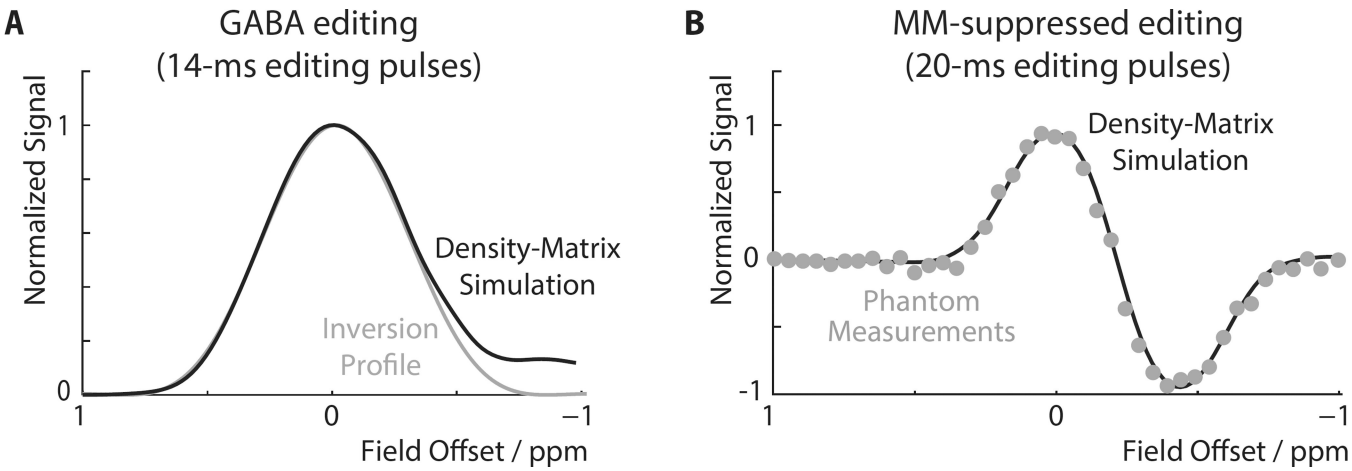

Figure 2.

B_0 Offset-dependence of GABA editing. (A) Full density-matrix simulation of the GABA signal as a function of B_0 offset (zero field offset = edit ON pulse at 1.9 ppm) using 14-ms editing pulses at TE = 68 ms. The signal profile has a single positive lobe with a maximum at zero offset. The inversion profile of the editing pulses is overlaid. (B) Full density-matrix simulations (solid line) and experimental data in the phantom (data points) for the MM-suppressed experiment applying editing pulses at 1.9 ppm (ON) and 1.5 ppm (OFF).

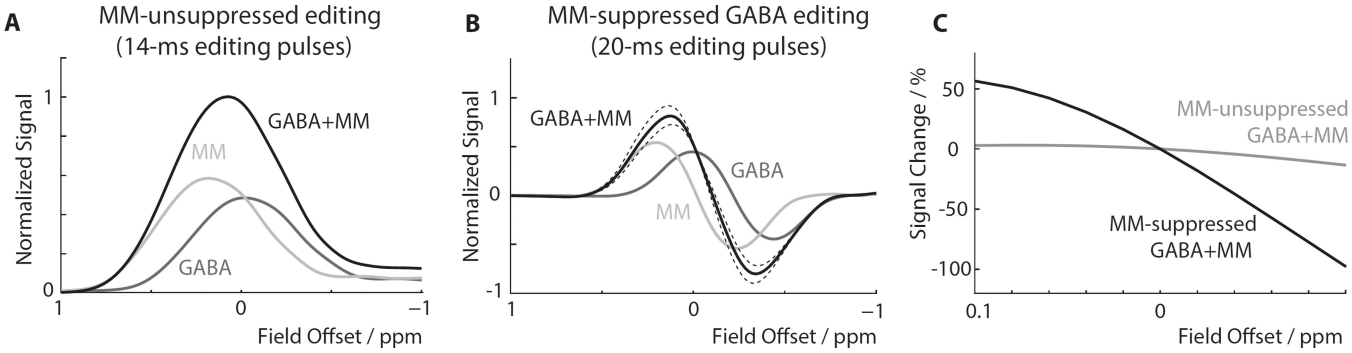

Figure 3.

Simulations of the B_0 field offset-dependence of GABA and MM. Normalization of the signal curves was performed with respect to the maximum total signal of the GABA+ experiment to allow for comparison between both editing schemes. (A) GABA and MM signals, as well as their sum (GABA+), are shown for the MM-unsuppressed experiment with 14 ms editing pulses. The relative amounts of GABA and MM are set to be equal at zero offset. (B) GABA and MM signals for the MM-suppressed acquisition with 20 ms editing pulses. The MM response to the MM-suppressed experiment shows a zero-crossing at zero field offset, as expected. As the field offset increases or decreases, the total observed signal will contain contributions from both GABA and MM, with either positive or negative MM contributions depending on the direction of the offset. The solid dark curve represents a 50:50 MM:GABA ratio; dashed lines indicate 45:55 and 55:45 ratios, respectively. (C) Percentage changes the MM-unsuppressed (from A) and MM-suppressed simulations (from B). It can be seen that the MM-suppressed signal changes much more rapidly (by about an order of magnitude) as a function of field offset.

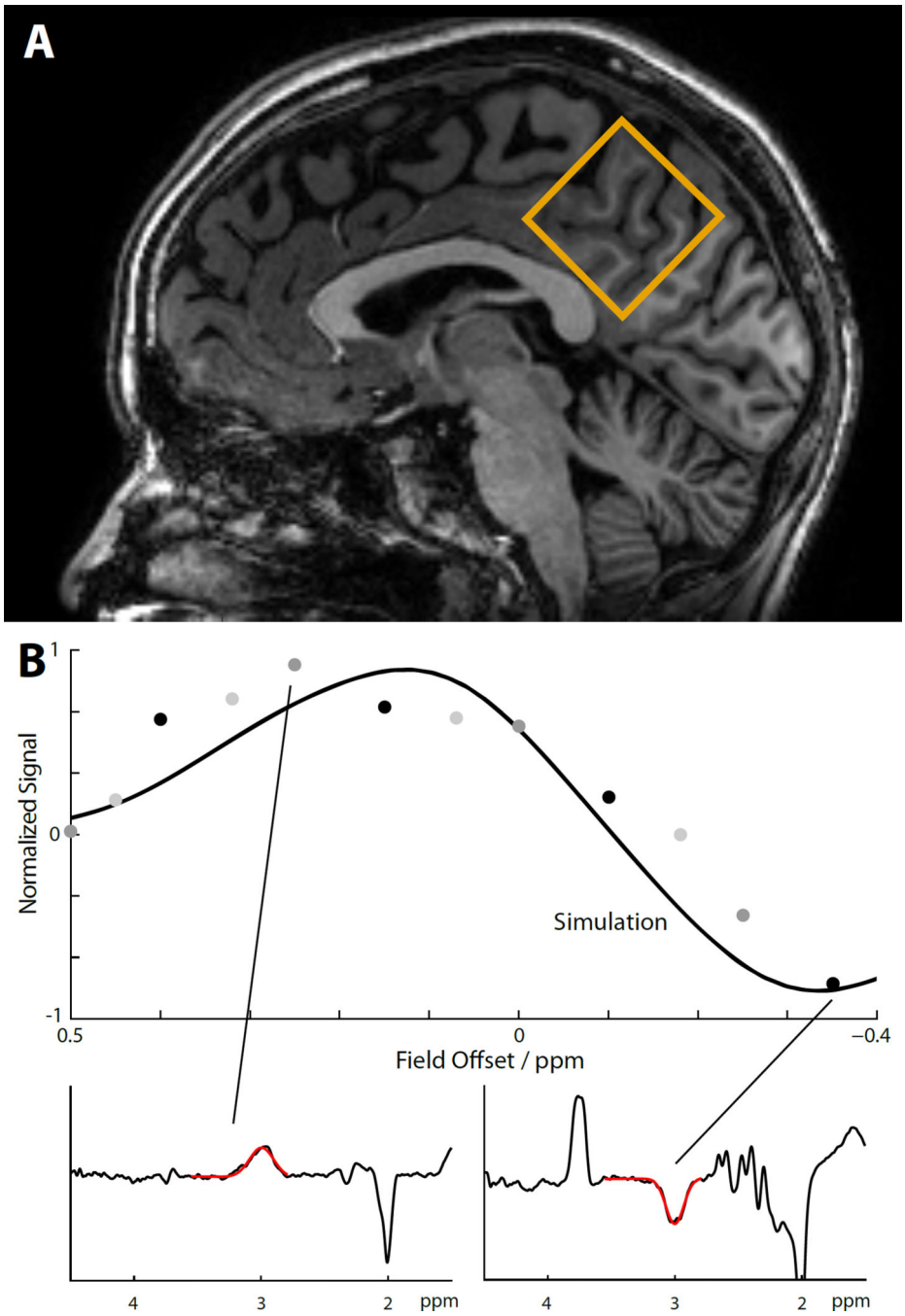

Figure 4.

Offset-dependence of MM-suppressed GABA experiments *in vivo*. (A) Midline parietal voxel (35×35×35 mm^3) from sagittal view. (B) Comparison of simulations and experimental *in vivo* measures for the total signal of the MM-suppressed experiment. The solid line shows the simulation pattern from Figure 3B for a 50:50 GABA:MM ratio, while experimental data points are indicated in gray and black (n=3, different shade of gray/black for each subject). The spectrum corresponding to a case of high positive field offset (+0.25 ppm) shows a large signal at 3 ppm due to co-editing of positive MM signal. The spectrum corresponding to a

case of high negative field offset (−0.35 ppm) shows a negative signal at 3 ppm due to negative GABA-editing and simultaneous co-editing of negative MM signal, as predicted by simulations and phantom measurements. The red overlays in the inset spectra show the results of the Gannet curve-fitting routine to determine the area of the 3.0 ppm peak.

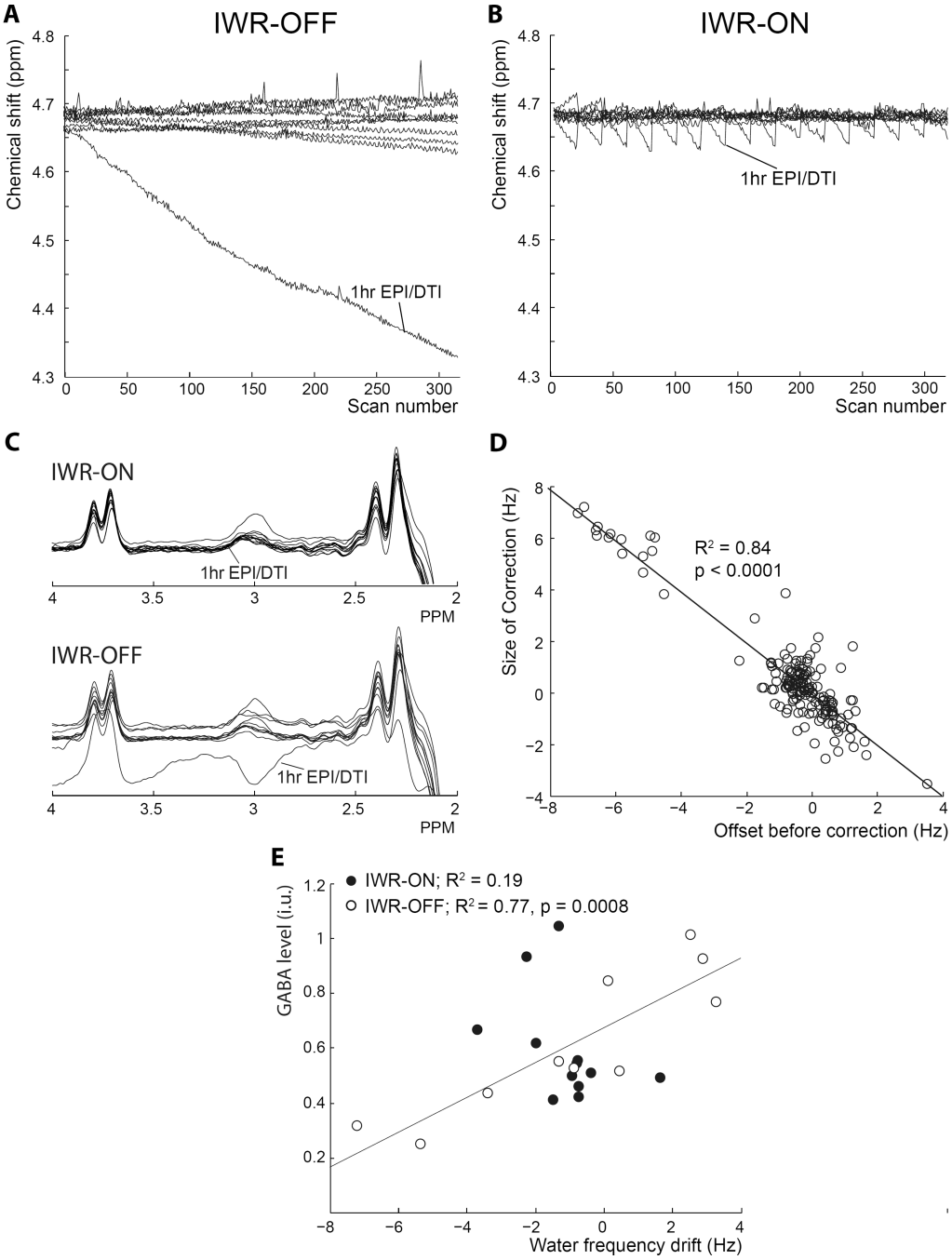

Figure 5.

Interleaved Water Reference-based (IWR) Frequency Stabilization. (A) and (B) plot the voxel water frequency for 12 subjects over the course of a 10 min 10 sec MEGA-PRESS acquisition (320 averages). In one of the subjects, a large field drift was observed due to a prior acquisition causing considerable gradient heating. Compared to conditions with no field-frequency lock applied (A), the IWR frequency stabilization (B) dramatically improves the offset behavior of the experiments. Vertical lines indicate the timing of interleaved F_0 updates. Since the field behavior is approximately linear in each segment, the stabilized

behavior resembles a sawtooth pattern. The two datasets (with and without IWR) in each panel were acquired sequentially in each subject, so the field behavior was similar (but not identical) in stabilized and non-stabilized scans. (C) MEGA-PRESS spectra from all 12 subjects plotted with and without IWR. It can be seen that the consistency of individual MEGA-PRESS spectra was substantially improved in data collected with IWR. (D) The frequency offset, measured in the spectrum one TR before the correction was made, is plotted against the size of the actual IWR correction applied. The perfect one-to-one relationship is indicated by the diagonal (slope: −1, intercept −0.027). (E) With IWR switched off, there is a strong correlation between mean field offset and measured GABA levels (white circles). With IWR switched on, this correlation is reduced (black circles).